Hydrogen absorption and lithium ion conductivity in Li$_6$NBr$_3$

Howard, Matthew; Clemens, O.; Slater, Peter; Anderson, Paul

Link to publication on Research at Birmingham portal

Accepted Manuscript

Hydrogen absorption and lithium ion conductivity in Li$_6$NBr$_3$

M.A. Howard, O. Clemens, P.R. Slater, P.A. Anderson

Hydrogen absorption and lithium ion conductivity in Li_6NBr_3

M.A. Howard [a], O. Clemens [a,b,c], P.R. Slater [a], P.A. Anderson [a,*]

[a] *School of Chemistry, University of Birmingham, Edgbaston, Birmingham B15 2TT, UK*

[b] *Technical University of Darmstadt, Joint Research Laboratory Nanomaterials, Jovanka-Bontschits-Straße 2, 64287 Darmstadt, Germany*

[c] *Karlsruhe Institute of Technology, Institute of Nanotechnology, Hermann-von-Helmholtz-Platz 1, 76344 Eggenstein-Leopoldshafen, Germany*

Corresponding author. Tel.: +44 121 414 4447; fax: +44 121 414 4403. E-mail address: p.a.anderson@bham.ac.uk (P.A. Anderson).

Abstract

The reaction of lithium amide and imide with lithium halides to form new amide halide or imide halide phases has led to improved hydrogen desorption and absorption properties and, for the amides, lithium ion conductivities. Here we investigate the effect of bromide incorporation on the ionic conductivity and hydrogen absorption properties of lithium nitride. For the first time we show that it is possible for a lithium halide nitride, the cubic bromide nitride Li_6NBr_3, to take up hydrogen—a necessary condition for potential use as a reversible solid-state hydrogen storage material. Powder X-ray diffraction showed the formation of $Li_2Br(NH_2)$ and $LiBr$, and Raman spectroscopy confirmed that only amide anions were present and that the hydrogen uptake reaction had gone to completion. The lithium ion conductivity of Li_6NBr_3 at the hydrogenation temperature was found to be less than that of Li_3N, which may be a significant factor in the kinetics of the hydrogenation process.

Keywords: hydrogen storage materials, lithium nitride, lithium bromide, lithium ion conductivity, powder X-ray diffraction, A.C. impedance spectroscopy

1. Introduction

The ability of many metals and alloys to absorb and store hydrogen has been known for many years [1], but the gravimetric hydrogen densities achieved are too low for many commercial applications. This has resulted in increased research into complex metal hydrides [2, 3]; however, even when these systems exhibit favourable thermodynamic properties for reversible hydrogen desorption, the kinetics of hydrogen desorption and/or absorption remain problematic.

Thermal decomposition of lithium amide ($LiNH_2$) produces ammonia (NH_3) rather than H_2, but the addition of lithium hydride (LiH) creates a pathway that can produce up to 10.3 wt% of hydrogen in two stages (Equation 1) [4, 5], though only the first stage (~6.5 wt%) has been regarded as useful for the reversible storage of hydrogen under practical conditions. Replacing $LiNH_2$ with magnesium

amide ($Mg(NH_2)_2$), which decomposes at a lower temperature than $LiNH_2$, results in a lower temperature of H_2 release [6].

$$LiNH_2 + 2LiH \leftrightarrow Li_2NH + H_2 + LiH \leftrightarrow Li_3N + 2H_2 \qquad (1)$$

More recent work has seen the incorporation of halides into $LiNH_2$ and lithium imide (Li_2NH), which also resulted in the release of H_2 at lower temperature than $LiNH_2$. Moreover, the resulting lithium imide halides required a lower temperature for hydrogen uptake compared to Li_2NH [7]. Interestingly, the most conducting of these, with room temperature ionic conductivities approaching 10^{-3} S cm^{-1}, were the quickest to release hydrogen on heating and to hydrogenate, and unwanted release of NH_3 was suppressed; it was suggested that improved lithium ion conductivity in the amide halide phases could be the reason for these improved hydrogenation properties [1]. The key role of NH_3 as an intermediate in the reaction between $LiNH_2$ and LiH was identified early on [8], but Borgschulte *et al.* [9] later showed that below 250°C the emission rate of NH_3 is sufficiently small that reversible dehydrogenation *via* a solid-state reaction may occur [10], controlled by the diffusion of ionic species such as Li$^+$ to or from LiH.

In comparison, the second stage of the dehydrogenation reaction has attracted comparatively little attention [11–13] as the relatively large reaction enthalpy results in a high temperature of desorption and the kinetics of the reverse reaction are slow. As part of our programme investigating the effect of halides on the ionic conductivity and hydrogen storage properties of lithium nitride (Li_3N), in this work we report results for the lithium bromide nitride phase Li_6NBr_3.

Li_6NBr_3 was first synthesized by Sattlegger and Hahn [14] in 1971, who reported an *fcc* structure with Li atoms being ordered in octahedra around the N atoms. This material was examined as a potential lithium ion conductor by Hartwig *et al.* [15]. Over 25 years after the original structural characterization by Sattlegger, Marx and Ibberson [16] used powder neutron diffraction to determine the Li distribution more accurately, but were unable to distinguish between two different possibilities: the first where the Li are disordered over distorted tetrahedral, and the second where they are disordered around the N atom in an octahedral configuration. Marx [17] , and Marx and Ibberson [16],

also studied phase changes that occurred at elevated and cryogenic temperatures. Here we report for the first time the hydrogenation of a lithium nitride halide and compare its hydrogen uptake properties to those of Li_3N.

2. Experimental

Lithium bromide nitride (Li_6NBr_3) was synthesized through direct solid state reaction of stoichiometric amounts of Li_3N (Sigma–Aldrich, 99.5% purity) and LiBr (Sigma–Aldrich, 99.999% purity), which were ground together in an agate pestle and mortar to achieve a homogeneous mixture. The ground powder was then transferred into a quartz tube lined with a metal (vanadium or nickel) sleeve. These manipulations were performed in an argon-filled glovebox to avoid contact with the atmosphere. The tube was evacuated under high vacuum, and sealed using an oxygen gas torch. The sealed tube was then heated at 430°C for 24 h followed by cooling down to ambient temperature, with heating and cooling rates of 50°C/h. Hydrogenations were performed for 24 hours in a high pressure hydrogenator under 90 bar H_2 at temperatures between 150–250°C. As a comparison Li_3N was hydrogenated under similar conditions.

For phase characterization, all powders were reground and packed into polyimide capillary tubes, which were sealed with an airtight adhesive. Powder X-ray diffraction (XRD) data were collected in the 2θ range 10–90° in capillary transmission geometry on a Siemens D5000 diffractometer with a $CuK_{\alpha 1}$ radiation source and position sensitive detector. The data were analysed using the TOPAS refinement suite [18].

For A.C. impedance spectroscopy measurements, Li_6NBr_3 powder was pressed into pellets under a load of 1 ton. The pressed pellets were sintered at 400°C for 3 h in evacuated quartz tubes, and the sintered pellets were then coated with silver to ensure good electrical contact at the surfaces and silver foil electrodes affixed. Typical sintered pellets were 6.9 mm in diameter, 1.0 mm thick with density ~83% of theoretical. A.C. impedance measurements were carried out under an argon atmosphere on a N4L PSM1735 phase-sensitive multimeter with impedance analysis interface. Equivalent circuits were used to calculate the resistance from the Nyquist plots. The impedance data showed a single

semicircle at the lowest temperature, with an additional spike seen at higher temperatures associated with the electrode response. For the semicircle, a single parallel circuit of R∥CPE was used as a model, indicating that it was not possible to resolve bulk and grain boundary components, and so the conductivities reported represent total conductivities.

Raman spectra were collected on a Renishaw inVia Raman microscope operating with a 633nm excitation laser. Samples were sealed inside airtight containers under an argon atmosphere.

3. Results and discussion

3.1 Synthesis of Li_6NBr_3

Li_6NBr_3 was synthesized as described above. A limited Rietveld refinement, where only unit cell parameters were refined, was carried out against powder XRD data obtained from the product using the structural model reported by Marx and Ibberson [16] (space group $Fm\bar{3}m$); experimental, calculated and difference profiles are shown in Figure 1. The lattice parameter refined to $a = 8.9334(1)$ Å, comparable to that previously reported of $a = 8.93896(4)$ Å.

3.2 Hydrogenation of Li_6NBr_3 and Li_3N

Hydrogenation of Li_6NBr_3 was attempted for 24 hours at temperatures between 150–250°C under 90 bar H_2. It was found that no hydrogenation occurred at temperatures lower than 250°C. At 250°C, the compound was found to hydrogenate to give Li_2NH_2Br and LiBr. It is expected that LiH was also produced in the hydrogenation reaction (see Equation 2), but this compound is often difficult to observe in powder XRD patterns owing to the low scattering factors of Li and H. Rietveld refinement of the unit cell parameters using the structural model of Li_2NH_2Br as reported by Barlage and Jacobs [19] (space group *Pnma*), and the rock salt structure for LiBr, resulted in values of $a = 12.4882(4)$ Å, $b = 8.0090(2)$ Å, $c = 6.3710(2)$ Å, which are comparable to those previously reported [19] for Li_2NH_2Br, $a = 12.484(2)$ Å, $b = 7.959(1)$ Å, $c = 6.385(1)$ Å. Experimental, calculated and difference profiles are shown in Figure 2a.

$$Li_6NBr_3 + 2H_2 \rightarrow Li_2NH_2Br + 2LiBr + 2LiH \qquad (2)$$
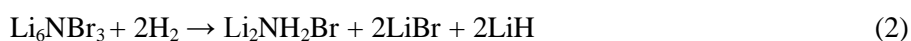
As it is possible that not all the products of hydrogenation were crystalline, Raman spectroscopy was used to examine if the hydrogenation reaction was complete. The Raman spectrum of the hydrogenated products (Figure 2b) shows at least three peaks at ~3220, 3245 and 3280 cm^{-1}. All of these are higher in frequency than imide stretching vibrations we have observed in lithium imide and a range of lithium imide halides (<2200 cm^{-1}) and are consistent with NH_2^- stretching modes and the observation of the amide Li_2NH_2Br as the main hydrogenation product in the powder XRD pattern. The broadness of the peaks observed between 3200–3250 cm^{-1} may be indicative of some disorder within the Li_2NH_2Br structure or possibly the presence of a secondary amorphous phase.

As a comparison Li_3N was hydrogenated under the same conditions; it was found that the nitride hydrogenated at lower temperature (150°C) than Li_6NBr_3.

3.3 A.C. impedance spectroscopy

The conductivity of Li_6NBr_3 was measured from 65–310°C. The Nyquist plot showed a single semicircle at high frequency (Figure 3a) assigned to total conductivity. The conductivity was calculated to be $\sigma_{(65°C)} = 1.86 \times 10^{-7} S\ cm^{-1}$, which is comparable to previous reports [15]. A temperature-dependent plot of the conductivity of Li_6NBr_3 is shown in Figure 3b; the activation energy was calculated from the line of best fit for data below 197°C to be 0.69(2) eV. Li_3N ionic conductivity was also measured as a comparison: at 250°C it was found to be $\sigma_{(250°C)} = 2.0 \times 10^{-2} S\ cm^{-1}$, which is more than 10 times higher than Li_6NBr_3 ($\sigma_{(250°C)} \approx 10^{-3} S\ cm^{-1}$).

It is interesting that Li_6NBr_3 was harder to hydrogenate under the conditions of our experiments than Li_3N. Thermodynamic data are not yet available for the bromide-containing phases, so a thermodynamic explanation for this cannot be discounted, but as the hydrogenated product is thermodynamically favoured at low temperatures in reversible systems, hydrogenation is in practice often kinetically limited. Hydrogen adsorption by Li_3N is strongly exothermic, so the observation that the absorption is thermally activated can only be explained by slow kinetics. It follows that these observations are consistent with the lower ionic conductivity of Li_6NBr_3 and the proposal that this is an important parameter in the kinetics of rehydrogenation [7, 9, 10].

The Li_3N structure consists of planar hexagonal layers of lithium cations each centred by a nitride anion. Each Li_6N hexagon is capped above and below the *ab* plane by further Li^+ ions to form a linear Li_2N coordination [20]. The structure of Li_6NBr_3 can be understood as a *ccp* arrangement of the Br^- ions at the 4a site, with the N^{3-} ions at 4b filling all of the octahedral holes and further Br^- ions at 8c filling all the tetrahedral holes, which clearly limits the amount of available space in the structure. Six lithium ions are located around N^{3-} to form an octahedron. For bulk lithium transport Li cations have to move from one nitride ion to a neighbouring one and must pass through a coordination environment, in which it would be coordinated to 4 Br^- ions only. This is likely to increase the energy of diffusion, thus explaining why the conductivity is lower in the Li_6NBr_3 system compared to Li_3N. A comparison of the structures of Li_6NBr_3, indicating the proposed diffusion pathway, and Li_3N is given in Figure 4.

4. Conclusion

Li_6NBr_3 was successfully synthesized through direct solid state reaction of Li_3N and $LiBr$. Powder XRD showed a diffraction pattern that matched previous reports with comparable lattice parameter and space group $Fm\bar{3}m$.

Powder XRD studies showed that Li_6NBr_3 can be hydrogenated at 250°C under 90 bar H_2 to give $Li_2Br(NH_2)$ and $LiBr$; Raman spectroscopy confirmed that only amide anions were present and that the hydrogenation had gone to completion. Under similar conditions it was found that hydrogenation of Li_3N occurred at significantly lower temperature than that of Li_6NBr_3. This observation is consistent with the lower ionic conductivity of Li_6NBr_3, as determined by A.C. impedance spectroscopy, and the proposal that this is an important parameter in the kinetics of rehydrogenation.

Figure List

Figure 1. Observed, calculated and difference Rietveld powder XRD profiles for Li_6NBr_3.

Figure 2. a) Observed, calculated and difference Rietveld powder XRD profiles for hydrogenated Li_6NBr_3 at 250°C under 90 bar H_2 (upper tick marks LiBr, lower tick marks Li_2BrNH_2) ; b) Raman spectrum of hydrogenated Li_6NBr_3.

Figure 3. a) Experimental (circles) and calculated (dashed line) Nyquist plot for Li_6NBr_3 at 197°C; b) Arrhenius plot for Li_6NBr_3 from 65–310°C.

Figure 4. Structures of a) Li_3NBr_3, with proposed pathway for lithium ion diffusion indicated by an arrow, and b) Li_3N.

**References**

[1] L. Schlapbach, A. Züttel, Hydrogen-storage materials for mobile applications, Nature 414 (2001) 353-358.

[2] B. Bogdanović, M. Schwickardi, Ti-doped alkali metal aluminium hydrides as potential novel reversible hydrogen storage materials, J. Alloys Comp. 253 (1997) 1-9.

[3] A. Züttel, P. Wenger, S. Rentsch, P. Sudan, P. Mauron, C. Emmenegger, $LiBH_4$ a new hydrogen storage material, J. Power Sources 118 (2003) 1-7.

[4] P. Chen, Z.T. Xiong, J.Z. Luo, J.Y. Lin, K.L. Tan, Interaction of hydrogen with metal nitrides and imides, Nature 420 (2002) 302-304.

[5] P. Chen, Z.T. Xiong, J.Z. Luo, J.Y. Lin, K.L. Tan, Interaction between lithium amide and lithium hydride, J. Phys. Chem. B 107 (2003) 10967-10970.

[6] W.F. Luo, ($LiNH_2$-MgH_2): a viable hydrogen storage system, J. Alloys Comp. 381 (2004) 284-287.

[7] P.A. Anderson, P.A. Chater, D.R. Hewett, P.R. Slater, Hydrogen storage and ionic mobility in amide-halide systems, Faraday Discuss. 151 (2011) 271-284.

[8] Y. H. Hu, E. Ruckenstein, Ultrafast Reaction between LiH and NH_3 during H_2 storage in Li_3N, J. Phys. Chem. A 107 (2003), 9737–9739.

[9] A. Borgschulte, M.O. Jones, E. Callini, B. Probst, S. Kato, A. Züttel, W.I.F. David, S.-I. Orimo, Surface and bulk reactions in borohydrides and amides, Energy Environ. Sci. 5 (2012) 6823-6832.

[10] W.I.F. David, M.O. Jones, D.H. Gregory, C.M. Jewell, S.R. Johnson, A. Walton, P.P. Edwards, A Mechanism for Non-stoichiometry in the lithium amide/lithium imide hydrogen storage reaction, J. Am. Chem. Soc. 129 (2007) 1594-1601.

[11] E. Weidner, D.J. Bull, I.L. Shabalin, S.G. Keens, M.T.F. Telling, D.K. Ross, Observation of novel phases during deuteration of lithium nitride from in situ neutron diffraction, Chem. Phys. Lett. 444 (2007) 76-79.

[12] D.J. Bull, E. Weidner, I.L. Shabalin, M.T.F. Telling, C.M. Jewell, D.H. Gregory, D.K. Ross, Pressure-dependent deuterium reaction pathways in the Li-N-D system, Phys. Chem. Chem. Phys. 12 (2010) 2089-2097.

[13] D.J. Bull, N. Sorbie, G. Baldissin, D. Moser, M.T.F. Telling, R.I. Smith, D.H. Gregory, D.K. Ross, In situ powder neutron diffraction study of non-stoichiometric phase formation during the hydrogenation of Li_3N, Faraday Discuss. 151 (2011) 263-270.

[14] H. Sattlegger, H. Hahn, Über das System $Li_3N/LiCl$, Z. Anorg. Allg. Chem. 379 (1971) 293-299.

[15] P. Hartwig, W. Weppner, W. Wichelhaus, A. Rabenau, Ionic transport in the lithium nitride bromides Li_6NBr_3 and $LI_{13}N_4Br$, Solid State Commun. 30 (1979) 601-603.

[16] R. Marx, R.M. Ibberson, Time-of-flight neutron diffraction study on the cryolite type phases of Li_6NBr_3, J. Alloys Comp. 261 (1997) 123-131.

[17] R. Marx, Time-of-flight neutron diffraction study on the Li_2O type phases of Li_6NBr_3, J. Alloys Comp. 256 (1997) 196-206.

[18] A.A. Coelho, Topas Academic v4.1 Computer Software, Brisbane, 2007.

[19] H. Barlage, H. Jacobs, $Li_2Br(NH_2)$ - The 1st ternary alkali-metal amide halide, Z. anorg. allg. Chem. 620 (1994) 479-482.

[20] D.H. Gregory, Nitride chemistry of the s-block elements, Coord. Chem. Rev., 215 (2001) 301-345.

$R_{exp} = 1.894\%$

$Li_2Br(NH_2)$ $R_{Bragg} = 1.754\%$

$LiBr$ $R_{Bragg} = 3.821\%$

$GOF = 2.515$
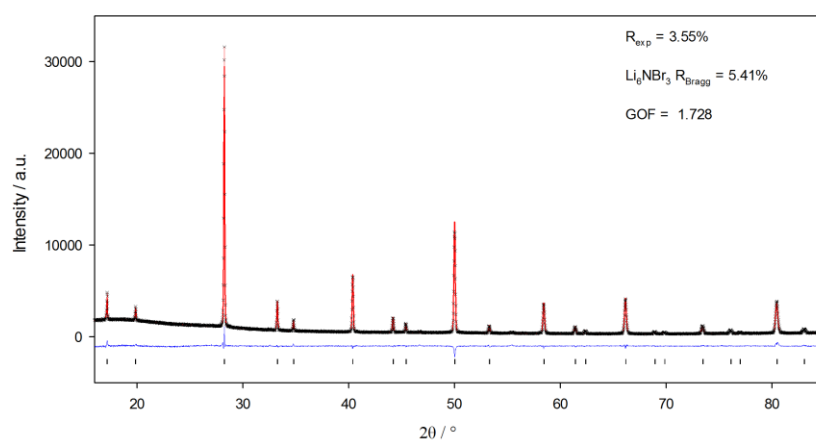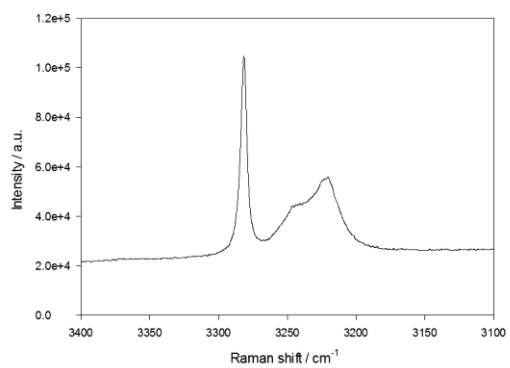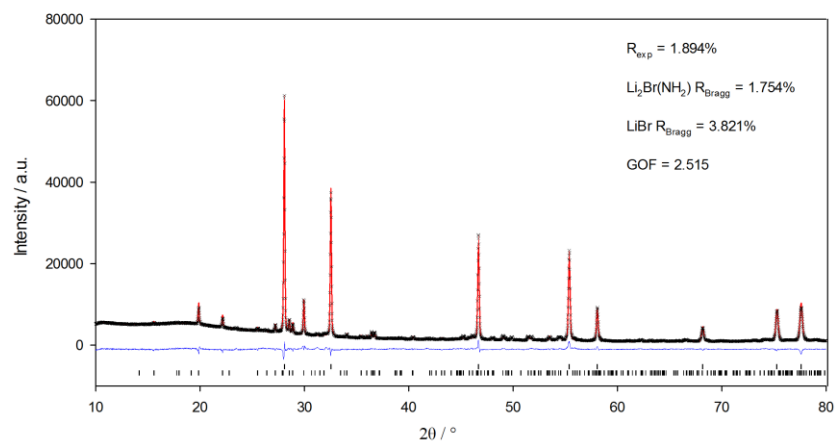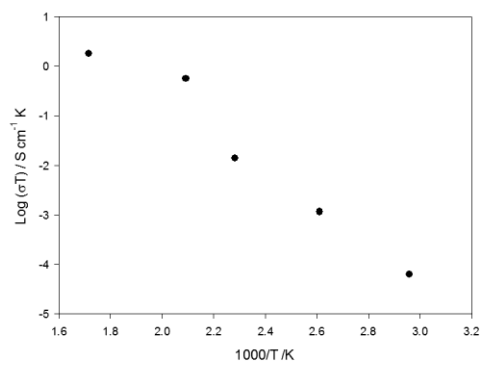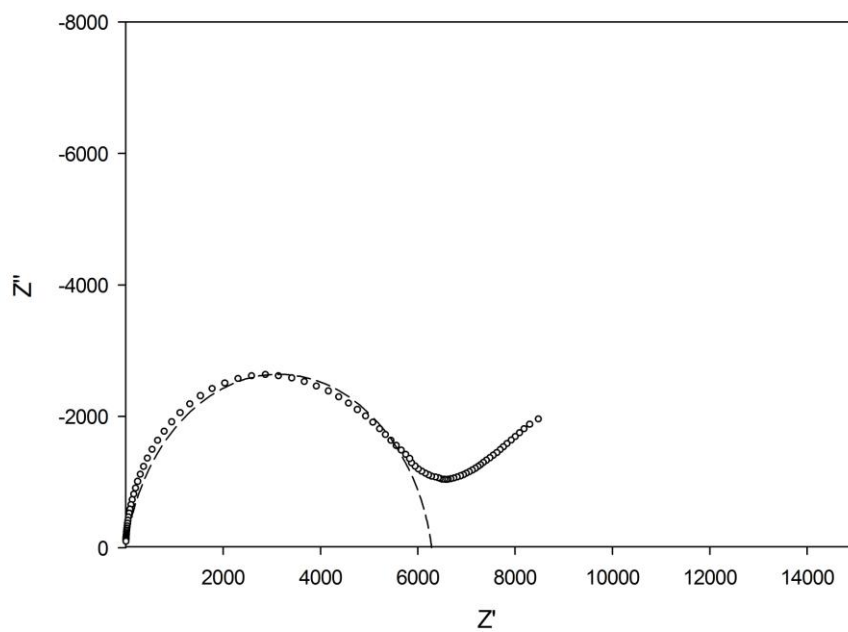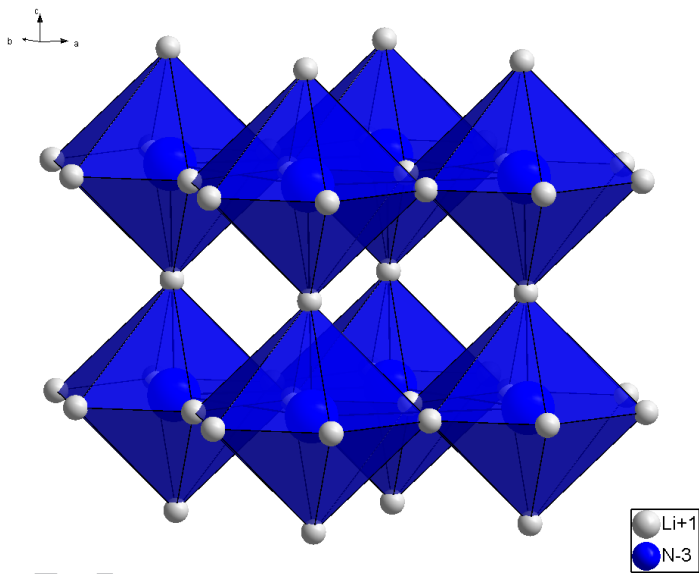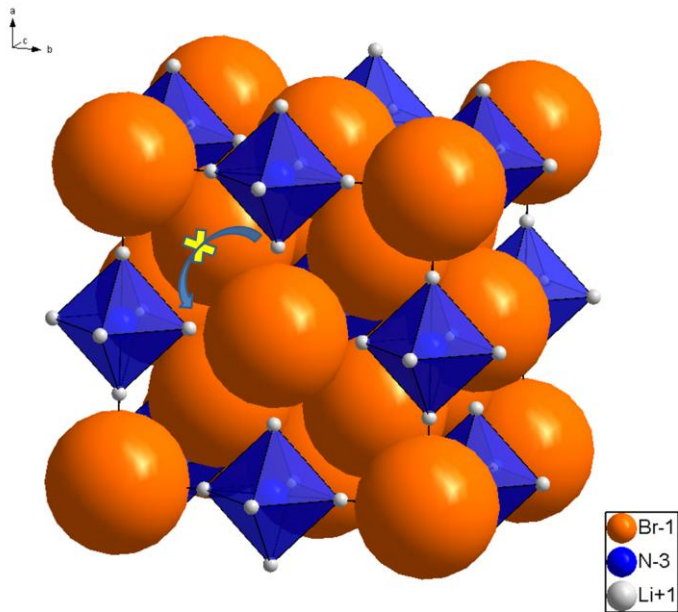
Highlights

- Li_6NBr_3 was synthesized *via* solid state methods and hydrogenation attempted.
- Hydrogenation of a lithium nitride halide was demonstrated for the first time.
- Powder XRD and Raman spectroscopy showed that hydrogenation had gone to completion.
- The ionic conductivities of Li_6NBr_3 and Li_3N were compared through A. C. impedance spectroscopy.
- The lower conductivity of Li_6NBr_3 is consistent with its higher hydrogenation temperature.